

Interaction of Fructose Dehydrogenase with a Sulfonated Polyaniline: Application for Enhanced Bioelectrocatalysis

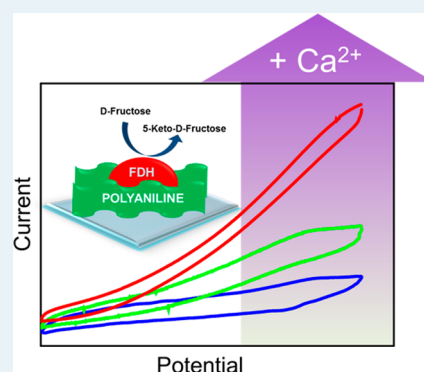
David Sarauli,^{*,†,‡} Christoph Wettstein,[†] Kristina Peters,[‡] Burkhard Schulz,[§] Dina Fattakhova-Rohlfing,[‡] and Fred Lisdat^{*,†}

[†]Biosystems Technology, Institute for Applied Life Sciences, Technical University of Applied Sciences Wildau, Hochschulring 1, D-15745, Wildau, Germany

[‡]Department of Chemistry and Centre for NanoScience (CeNS), University of Munich (LMU), Butenandtstraße 5-13 (E), D-81377, Munich, Germany

[§]Institute for Thin Film and Microsensor Technologies, Kantstraße 55, D-14513 Teltow, Germany

ABSTRACT: We report on efficient bioelectrocatalysis of the redox enzyme fructose dehydrogenase (FDH) upon its interaction with the sulfonated polyaniline PMSA1 (poly(2-methoxyaniline-5-sulfonic acid)-*co*-aniline). This interaction has been monitored in solution and on the surface of planar and macroporous indium tin oxide (ITO) electrodes by UV–vis and cyclic voltammetric measurements. Moreover, an enhancement of the catalytic activity for fructose conversion induced by a structural change of sulfonated polyaniline PMSA1 caused by the presence of Ca^{2+} ions is observed. An entrapment of the Ca^{2+} -bound polymer and enzyme inside the pores of macroporous ITO electrodes leads to a significantly increased (~ 35 -fold) bioelectrocatalytic signal in comparison to that of a flat ITO and allows the fabrication of highly efficient electrodes with good stability.



KEYWORDS: bioelectrocatalysis, fructose dehydrogenase, sulfonated polyanilines, ITO electrodes, entrapped enzyme

INTRODUCTION

Fabrication of electronic devices based on biomolecules such as proteins, enzymes, antibodies, or DNA fragments has attracted continuing attention due to the unprecedentedly high efficiencies and selectivities of biological systems. One of the major challenges for the commercial development of bioelectronic devices such as biosensors and biofuel cells is the implementation of biomolecules into electronic circuits, ensuring the complete retention of their biological properties.^{1–8} Contacting biomolecules with electrode surfaces modified with conductive, conjugated polymers has become widely used for the construction of sensing units with electrochemical or optical readout. Even though the concept of direct polymer/biomolecule wiring is not new, only a limited number of functional systems, including the enzymes alcohol dehydrogenase, laccase, and pyrroloquinoline quinone dependent glucose dehydrogenase (PQQ-GDH), entrapped into polypyrrole, thiophene, or polyaniline have been demonstrated.^{9–13}

The redox enzyme D-fructose dehydrogenase (FDH; EC 1.1.99.11) from *Gluconobacter japonicus* (formerly *Gluconobacter industrius*)¹⁴ catalyzes the oxidation of D-fructose to produce S-keto-D-fructose. Due to its strict substrate specificity to D-fructose,¹⁵ it is widely used for the development of biosensors and biofuel cells.^{16–18} FDH is a heterotrimeric membrane-bound enzyme with a molecular mass of ca. 140 kDa, consisting of subunits I (67 kDa), II (51 kDa), and III (20

kDa). The enzyme is a flavoprotein–cytochrome *c* complex, since subunits I and II contain covalently bound flavin adenine dinucleotide (FAD) and heme C as prosthetic groups, respectively.¹⁹ FDH allows a direct electron transfer (DET) type bioelectrocatalysis,^{20,21} which strongly depends on the electrode material. However, until now no report on contacting FDH with the help of conducting polymers capable of enhancing its bioelectrochemical activity has been known.

We demonstrate here a FDH-based tunable bioelectrocatalytic system by entrapping the enzyme into a sulfonated polyaniline matrix on transparent electrode surfaces. Sulfonated polyanilines have already been established as materials suitable for the construction of different sensing electrodes as e.g. for detection of DNA hybridization^{22,23} or low-molecular-weight compounds such as oxalate and organophosphate.^{24,25} This is mainly due to their high conductivity in comparison to nonsubstituted polyanilines together with other advantages such as improved solubility and redox activity over a wide pH range.^{26–31} Moreover, sulfonated polyanilines have been used in our group as building blocks for the design of novel multilayer architectures with cytochrome *c* only^{32,33} and cytochrome *c* with xanthine oxidase,³⁴ bilirubin oxidase,^{35,36} and sulfite oxidase.³⁷

Received: January 22, 2015

Revised: February 16, 2015

Published: February 18, 2015

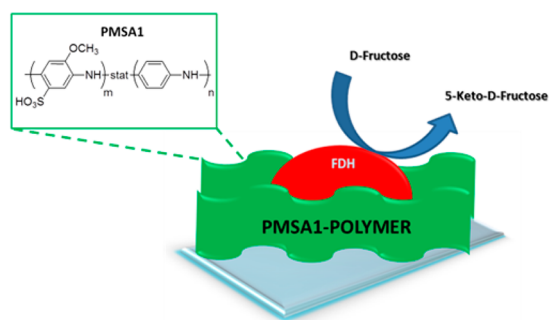
It has also been demonstrated that the sulfonated polyaniline copolymer PMSA1, containing a 2-methoxyaniline-5-sulfonic acid (MAS) monomer, is not only able to react directly with PQQ-GDH³⁸ but can also serve as an immobilization matrix without inhibiting the catalytic activity of the entrapped enzyme on gold,¹¹ planar ITO,¹¹ and macroporous ITO electrodes.¹⁰ The polymer acts here as a conducting environment helping to close the enzymatic cycle by withdrawing electrons from the substrate-reduced enzyme.

In this study the interaction between the sulfonated polyaniline PMSA1 and FDH has been initially monitored in solution. The unprecedented enhancement of the catalytic reaction has been demonstrated upon addition of Ca²⁺ ions to the polymer/enzyme solution in the presence of the substrate fructose. Exploiting this interaction, a new, tunable, and shuttle-free biohybrid system on electrodes has been constructed. For this purpose the enzyme has been entrapped into polymer films on indium tin oxide (ITO) and on the 3D structure of macroporous indium tin oxide (macroITO) electrode surfaces. The influence of Ca²⁺ ions on the polymer and the efficiency of the electron transfer with free and immobilized FDH is discussed.

RESULTS AND DISCUSSION

Polymer Enzyme Reaction in Solution. Scheme 1 demonstrates the construction principle of our polymer/

Scheme 1. Schematic Illustration of the Polymer-Based Enzyme Electrode Architecture



enzyme electrode. One prerequisite for the successful development of a functional and stable polymer/enzyme electrode system is an efficient electron transfer between the enzyme and the chosen polymer. Therefore, the interaction between PMSA1 and FDH has been first monitored in solution. For this purpose UV–vis spectroscopy measurements at different pH values (pH range 4.0–6.5) have been performed. The pH range has been chosen according to optimum pH values reported in the literature for the enzyme.^{19,39,40}

At these pH values PMSA1 polymer exists in its emeraldine salt (ES) oxidation state after synthesis.³⁸ Figure 1 illustrates the spectral changes occurring after addition of the substrate fructose to a solution containing a mixture of PMSA1 and FDH at pH 5.5. Two characteristic bands at 325 and 469 nm (curve 1) can be assigned to π – π^* transitions and to a low-wavelength polaron band, respectively. They are characteristic of the ES state.³⁸ Upon addition of fructose strong bands at 330 and 393 nm appear, whereas the low-wavelength polaron band slightly shifts to 463 nm with decreased intensity. It seems that the electronic structure of PMSA1 is changed due to partial polymer reduction upon the enzymatic conversion of fructose,

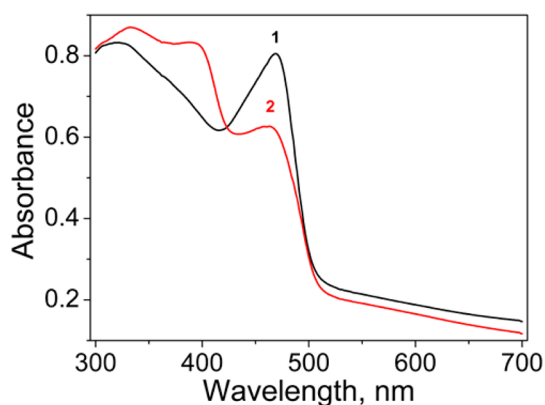


Figure 1. UV–vis spectra of PMSA1 with FDH in the absence (1) and in the presence (2) of the substrate fructose. Experimental conditions: [PMSA1] = 40 $\mu\text{g/mL}$, [FDH] = 18 $\mu\text{g/mL}$, [fructose] = 100 mM in 10 mM MES buffer at pH 5.5, $t = 25^\circ\text{C}$.

demonstrating the ability of PMSA1 to act as a reaction partner for FDH.

In order to gain an insight into the nature of the polymer–enzyme interaction, the overall charge on both reacting species has to be taken into account. Since the isoelectric points of both sulfonated polyaniline and FDH are determined to be $pI < 5.0$,⁴¹ it is evident that at $pH > 5.0$ both species are negatively charged in solution, so that an electrostatic repulsion between the polymer and the FDH can be expected. Therefore, we have tested whether the interaction between the polymer and the enzyme can be tuned by changing the charge of PMSA1. One approach would be the use of Ca²⁺ ions, since it has been reported that they can coordinate to SO₃[−] groups on aniline rings in emeraldine salt polyanilines, partially screening the electrostatic repulsions between SO₃[−] negative charges along the chains.^{42,43} Moreover, recently we have reported about the ability of Ca²⁺ ions to support the electrostatic interaction of two sulfonated polyanilines to form multilayer structures.¹¹ Therefore, the spectroscopic properties of PMSA1 in the presence of different Ca²⁺ amounts are the first to be clarified.

Figure 2a demonstrates the overall change in UV–vis absorbance of polymer PMSA1 upon addition of increasing Ca²⁺ concentrations. A clear decrease of absorbance at 469 nm together with the appearance of a distinct band at 393 nm and a small increase in absorbance at wavelength > 600 nm ($[\text{Ca}^{2+}] > 200$ mM) can be followed. These results confirm that there is a strong interaction between calcium ions and the polymer chains, showing saturation at higher calcium concentrations (Figure 2b).

To analyze the polymer changes, one should take into account that the self-doped polyanilines are known for their switching among completely oxidized (pernigraniline), half-oxidized (emeraldine), and completely reduced (leucoemeraldine) redox states.^{43–45} The oxidation state strongly influences the conductivity and reactivity of polyanilines, whereas the highest conductivity can be ensured in the emeraldine state (ES).^{46,47} Furthermore, interactions between different metal cations with sulfonate moieties of polyanilines have been reported by several groups.^{43,48–50} On the basis of their spectroscopic observations two polymer conformations have been supposed, even though no structural confirmations have been provided.^{43,48–50} According to these findings, we hypothesize that the spectroscopic features in Figure 2b are due to the change in different PMSA1 conformations (usually

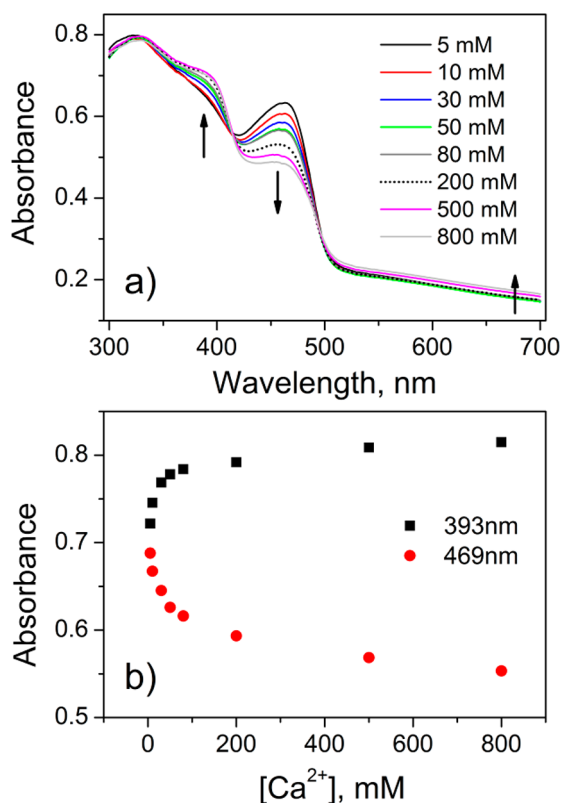


Figure 2. (a) Overall absorbance change of PMSA1 upon addition of different Ca^{2+} concentrations (from 5 to 800 mM). (b) Change in absorbance at 393 and 469 nm. Experimental conditions: $[\text{PMSA1}] = 40 \mu\text{g/mL}$ in 10 mM MES buffer at pH 5.5.

referred to as “extended coil” and “compact coil”), in line with existing arguments in the literature.^{43,48–50}

The question that arises in this respect is whether the change in the polymer can affect its interaction with the enzyme FDH. For this purpose the same experimental conditions as in our starting measurements (Figure 1) have been kept, except of the addition of $[\text{Ca}^{2+}] = 20 \text{ mM}$ to the solution of PMSA1, enzyme, and substrate. This calcium concentration corresponds to the end of the linear range of Ca^{2+} -dependent absorbance changes of PMSA1 as depicted in Figure 2b. The addition of 20 mM of Ca^{2+} to the polymer/enzyme/fructose solution drastically changes the absorption spectrum (Figure 3a, curve 3). However, this spectrum cannot be unambiguously attributed to the completely reduced form of PMSA1.^{38,43} It may rather represent a superimposed spectrum resulting from two different effects depicted in Figures 1 and 2a. In order to get a more detailed insight into whether the presence of calcium ions changes the interaction with the enzyme, we have carried out cyclic voltammetry measurements under the same experimental conditions.

Cyclic voltammetric measurements (Figure 3b) have been performed on ITO electrodes with the polymer and enzyme in solution. The electrochemical response of the mixed solution of PMSA1 and FDH (curve 2) without fructose results in the appearance of a weak redox couple with a formal potential of $+0.25 \pm 0.05 \text{ V}$ vs Ag/AgCl as reported before.^{10,45,51–53} After addition of fructose an oxidative bioelectrocatalytic current is observed starting slightly below 0 V vs Ag/AgCl, indicating an electron flow toward the ITO surface. It reaches a value of $\Delta I = 150 \text{ nA}$ at $E = +0.35 \text{ V}$ vs Ag/AgCl. Furthermore, the addition

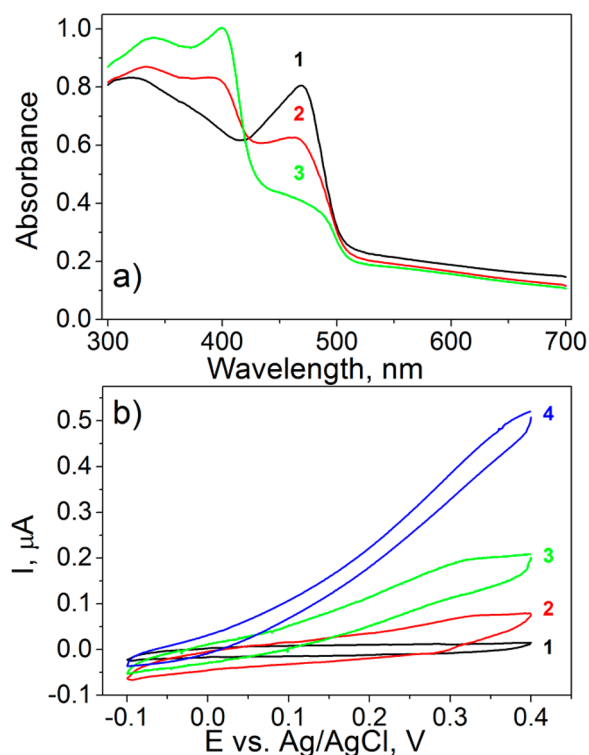


Figure 3. (a) UV-vis spectra of PMSA1 with FDH in the absence (1) and in the presence of fructose (2) together with the added Ca^{2+} (3). (b) CV of blank ITO electrode (1) and ITO electrode immersed in solution of PMSA1 + FDH without addition (2) and after addition (3) of fructose. Curve 4 corresponds to system 3 after addition of 20 mM Ca^{2+} . Experimental conditions: $[\text{PMSA1}] = 40 \mu\text{g/mL}$, $[\text{FDH}] = 18 \mu\text{g/mL}$, $[\text{Ca}^{2+}] = 20 \text{ mM}$, $[\text{fructose}] = 100 \text{ mM}$ in 10 mM MES buffer at pH 5.5, $t = 25 \text{ }^\circ\text{C}$, scan rate 5 mV/s.

of 20 mM Ca^{2+} results in a significant (3-fold) enhancement of the bioelectrocatalytic current ($\Delta I = 450 \text{ nA}$ at $E = +0.35 \text{ V}$ vs Ag/AgCl). These results clearly support the idea of an enhanced catalytic activity in the presence of Ca^{2+} , as indicated by the photometric measurements. However, it is not clear whether this fact originates from the improved interaction of the enzyme and the polymer or from an enhanced enzymatic conversion of fructose. Consequently, we have investigated this in more detail.

Since the electrochemical experiments clearly verify that the polymer can accept electrons from the enzyme, UV-vis was used to follow the reaction. Figure 4a summarizes pH-dependent initial rates of the polymer reduction in the presence and in the absence of 20 mM Ca^{2+} , demonstrating a significant (2.5-fold) increase in the reaction rate in comparison to the Ca^{2+} -free conditions. However, in order to attribute the enhanced polymer reduction to the calcium-supported interaction between the polymer and the FDH, the activity of the enzyme in dependence on the Ca^{2+} concentrations needs to be studied in the absence of the polymer. We have performed the measurements of the enzyme activity according to the established assay (see the Experimental Section) in the presence of increasing Ca^{2+} concentrations (see Figure 4a). Clearly visible is an increase in enzymatic activity of FDH in the presence of Ca^{2+} . However, this increase is much smaller than that observed for the FDH-polymer reaction, being only about 1.45-fold of the activity in Ca^{2+} -free buffer. This means that the increase in reaction efficiency exemplified in Figure 4a and from

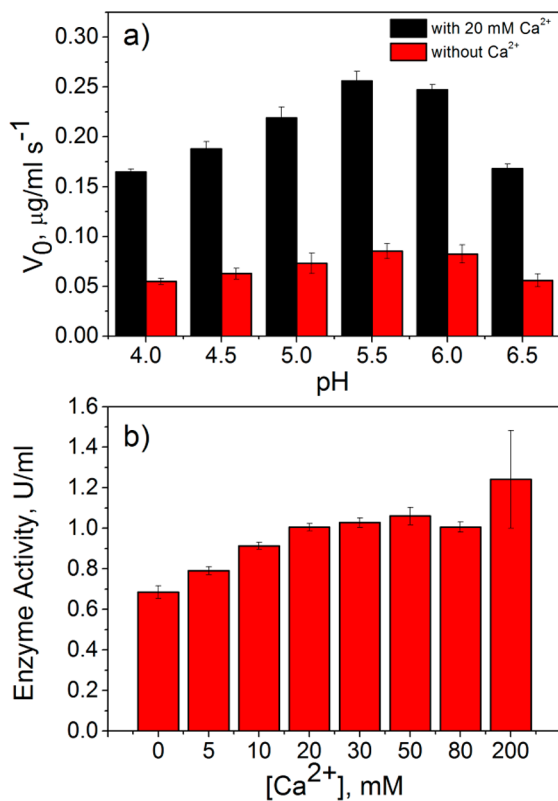


Figure 4. (a) pH-dependent initial rate V_0 of polymer reduction in the presence of FDH, fructose, and Ca²⁺ (measured by UV-vis). The reduction was measured at 408 nm. The rate was calculated from the time-dependent absorbance change according to the Lambert–Beer equation using the extinction coefficients of oxidized and reduced polymers. (b) Determination of the enzyme activity according to Ameyama¹⁹ with increasing Ca²⁺ concentrations at pH 5.5. Experimental conditions: [polymer] = 40 μg/mL, [FDH] = 18 μg/mL, [fructose] = 100 mM in 10 mM MES buffer.

the electrochemical measurements (Figure 3b), which show a 2.5-fold enhancement, can be mainly attributed to the improved interaction of the enzyme with the Ca²⁺-bound polymer.

Application of PMSA1–FDH Reaction for the Construction of Enzyme Electrodes. In the next step of the study we have investigated whether it is possible to build efficient enzyme electrodes using the PMSA1 polymer and FDH, exploiting hereby the enhanced interaction in the presence of Ca²⁺ ions. For this purpose the approach of enzyme entrapment has been chosen in order to ensure a good stability of the system. First, planar ITO electrodes have been modified with a PMSA1 film and entrapped FDH.

The electrode modification has been performed by adsorption from polymer/enzyme solutions in the absence and in the presence of Ca²⁺ ions. Cyclic voltammograms of the ITO/(PMSA1:FDH) electrode incubated in a Ca²⁺-free buffer solution (Figure 5a, curve 1) without fructose are similar to those observed in solution, with one weak redox couple at $E = +0.25 \pm 0.05$ V vs Ag/AgCl attributed to the PMSA1 conversion. After addition of fructose (curve 2) bioelectrocatalytic currents are observed, giving proof of the presence of the electroactive enzyme in the film. The catalytic current starts at $E = 0$ V vs Ag/AgCl, reaching the value of $\Delta I = 15$ nA at $E = +0.35$ V vs Ag/AgCl. After addition of 20 mM Ca²⁺ (curve 3) a clearly enhanced bioelectrocatalytic current with $\Delta I = 35$ nA at

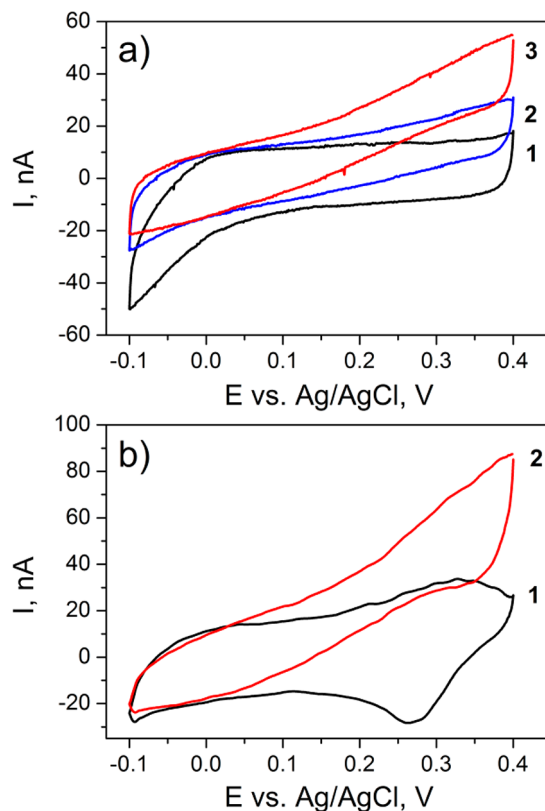


Figure 5. CVs of (a) ITO/(PMSA1:FDH) immobilized in Ca²⁺-free solution (1), after addition of fructose (2), and after consequent addition of 20 mM of Ca²⁺ (3) and (b) ITO/(PMSA1:FDH) immobilized in the presence of Ca²⁺ (1) and in the presence of fructose (2). Experimental conditions: [fructose] = 100 mM in 10 mM MES buffer with or without 20 mM CaCl₂ at pH 5.5, $t = 25$ °C, scan rate 5 mV/s.

$E = +0.35$ V vs Ag/AgCl appears. This is in agreement with measurements in solution (Figure 3b); however, the catalytic current intensities are significantly smaller.

Cyclic voltammograms of the ITO/(PMSA1:FDH) electrode prepared in the presence of Ca²⁺ in MES buffer solution (Figure 5b, curve 2) demonstrate a higher bioelectrocatalytic response after addition of fructose, since the value of $\Delta I = 48$ nA at $E = +0.35$ V vs Ag/AgCl can be reached. This fact can be easily explained by a long incubation time (2 h), during which time Ca²⁺ ions are expected to bind to the SO₃⁻ groups on PMSA1, and thus the enzyme is coimmobilized with the Ca²⁺-bound polymer for better interaction. Therefore, we are able to see the enhancement of the polymer–enzyme reaction also on ITO electrodes. It has to be emphasized here that in this case efficient bioelectrocatalysis has been observed by measuring the electrodes in buffer solution containing no free Ca²⁺ ions. Moreover, the starting potential of the bioelectrocatalytic fructose conversion is in agreement with the enzyme conversion on various electrode surfaces reported by Kano.^{20,21}

Efficient bioelectrocatalysis has also been observed with PQQ-GDH immobilized on different surfaces with sulfonated polyanilines.^{10,38,54–56} This was shown to proceed via a direct electron transfer pathway, even though interpretations of the reaction mechanism in the literature are controversial.⁵⁷ In order to evaluate whether a surface layer works as a mediator, one has to consider the formal potentials of the redox

conversions of different components of the system. The sulfonated polyanilines are redox active, although the peaks in the immobilized state are sometimes rather weak. When a bioelectrocatalytic current would be observed at potentials corresponding to the redox potential of the polymer, indicating that the oxidation process of the polymer triggers the bioelectrocatalysis, mediation can be concluded. However, when the bioelectrocatalysis is observed at much lower potentials, a direct electron transfer mechanism is valid, exploiting the conducting properties of the polymer. For PQQ-GDH at polymer-modified electrodes the catalytic current starts at about -0.1 V vs Ag/AgCl—far below the redox peaks of the polymer ($+0.05$ and $+0.2$ V vs Ag/AgCl).³⁸ The starting potential of the electrocatalytic currents on the FDH–polymer electrode is also rather low (~ 0 V vs Ag/AgCl), also suggesting a direct electron transfer pathway for this system. The rather similar starting potentials for different enzymes may be attributed in the first row to the conductivity of sulfonated polyanilines. Consequently, also reports on the polymer-supported bioelectrocatalysis of PQQ-dependent alcohol dehydrogenase and PQQ-dependent aldehyde dehydrogenase need to be reconsidered, since redox activity is found at potentials of about $+0.2$ mV vs Ag/AgCl, but catalysis already starts at potentials of about $+0.05$ mV vs Ag/AgCl.⁵⁷ It should also be noted here that the addition of Ca^{2+} cations generally increases the bioelectrocatalytic activity of PQQ-containing enzymes,⁵⁸ but FDH is a FAD-containing enzyme, which was independently studied in the present report.

In order to enhance the efficiency of the bioelectrocatalysis of FDH, 3D macroporous ITO electrode structures have been used. These materials have attracted great interest in recent years, since they can accommodate a largely increased amount of catalyst, resulting in enhanced signal generation. We have used a macroporous ITO electrode with a thickness of the porous ITO layer of about $1.2 \mu\text{m}$ and a pore size of 300 nm (Figure 6b,c), allowing a good access of polymer and enzyme to the inner surface during the immobilization and substrate molecules during operation. The macroporous ITO electrodes are incubated with a PMSA1/FDH mixture containing a medium concentration ratio of 1.5 mg mL^{-1} PMSA1/ $18 \mu\text{g mL}^{-1}$ FDH (see the Experimental Section). This concentration has been selected on the basis of the variation of the polymer/enzyme ratio, which demonstrates that there is only a limited concentration range in which bioelectrocatalysis occurs. At polymer concentrations higher than 1.5 mg mL^{-1} rather small catalytic currents can be detected. SEM micrographs after immobilization of the polymer/enzyme system have shown that the 3D structure was not affected by the treatment with the polymer–enzyme mixture.

Figure 6a shows cyclic voltammograms in Ca^{2+} -free buffer solution of a macroITO/(PMSA1:FDH) electrode prepared in the presence of Ca^{2+} ions, which are recorded in the absence (1) and in the presence (2) of fructose. A redox couple at $E = +0.25 \pm 0.05$ V vs Ag/AgCl attributed to the PMSA1 conversion is clearly observed. Upon addition of fructose to the buffer solution, the macroITO/(PMSA1:FDH) electrode exhibits an efficient bioelectrocatalytic current. The catalytic current starts from a potential of about $E = 0$ V vs Ag/AgCl and reaches at $+0.35$ V a value of $\Delta I = 1.6 \pm 0.2 \mu\text{A}$, with $n = 3$ (Figure 6a, curve 2). In addition, for this electrode architecture we can state that the oxidation process at $+0.25$ V vs Ag/AgCl is not necessary to collect the electrons from the enzyme. The bioelectrocatalysis demonstrates the efficient electron exchange

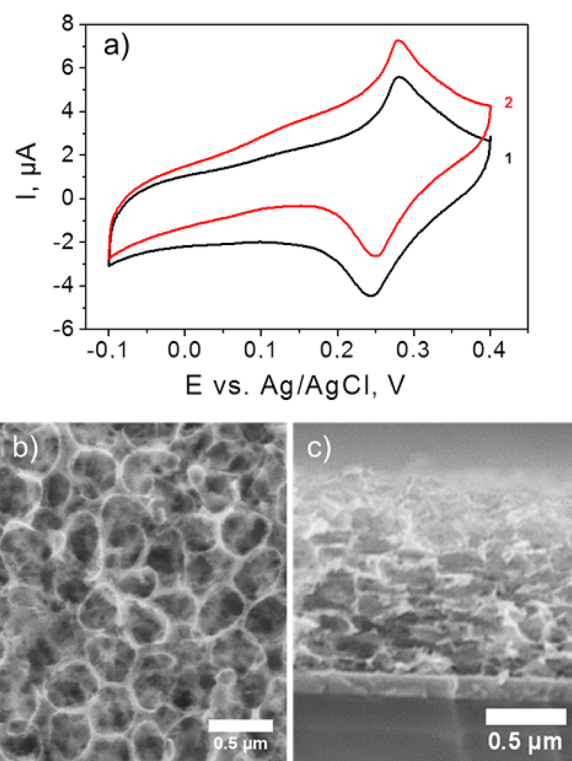


Figure 6. (a) CVs of macroITO/(PMSA1:FDH) immobilized in the presence of Ca^{2+} (1) and in the presence of fructose (2). Experimental conditions: [fructose] = 100 mM in 10 mM MES buffer with 20 mM CaCl_2 at $\text{pH } 5.5$, $t = 25 \text{ }^\circ\text{C}$, scan rate 5 mV/s . (b) Top view and (c) cross-section SEM images of the 3D macroporous ITO electrodes.

between a redox center of the entrapped enzyme and the accessible porous conductive electrode surface, indicating that the polymer environment inside the macroITO pores ensures the catalytic activity of FDH and allows efficient electron withdrawal from the reduced enzyme. However, at this point it cannot be stated which redox center is involved in the reaction with the polymer electrode. Since redox potentials of heme *c* moieties of FDH have been recently reported to be 10 ± 4 , 60 ± 8 , and $150 \pm 4 \text{ mV vs Ag/AgCl}$,²¹ the heme involvement is highly probable, but interaction with the FAD subunit cannot be excluded.

On comparison of the catalytic currents of the macroporous FDH electrodes with those on planar ITO (Figure 5b), a significant improvement of the bioelectrocatalytic properties of the system can be demonstrated, since a 35-fold increase in the catalytic current is achieved. This value is in good agreement with the almost 40 times higher electroactive area of the porous macroITO in comparison to that of the flat ITO, as determined from the analysis of the voltammetric charging current of both electrodes in a pure buffer solution (measured at a scan rate of 50 mV/s).

Because long-term stability is an important parameter for evaluation of the performance of a detection system, we have traced the stability of our macroITO/(PMSA1:FDH) electrodes by testing their activity in a fructose solution, after the electrodes have been kept at $4 \text{ }^\circ\text{C}$ in 10 mM MES + 20 mM CaCl_2 , $\text{pH } 5.5$, when not in use. The catalytic current response maintains over 50% of the initial value after 4 days, demonstrating that the entrapment of FDH in the sulfonated polyaniline films within the macroporous electrodes leads to a good retention of activity. Thus, our biohybrid system

developed by making use of a sulfonated polyaniline and its interaction with FDH and combination with macroporous 3D structures is a promising candidate to be used for biosensorial purposes.

CONCLUSION

We have demonstrated that an interaction between the sulfonated polyaniline PMSA1 and the redox enzyme FDH occurs in solution and on the electrodes, enabling the fabrication of efficient FDH-based bioelectrocatalytic systems. Moreover, an unprecedented enhancement of the catalytic activity of the redox enzyme FDH has been found—induced by the coordination of Ca^{2+} ions to sulfonic acid groups on the aniline ring of PMSA1.

Further developments have been performed by coimmobilization of FDH and the polymer on flat and macroporous ITO structures. This has allowed the construction of efficient enzyme electrodes with a good stability. The magnitude of FDH bioelectrocatalysis can already be tuned during the immobilization process by exploiting the calcium–polymer interaction and 3D electrode structures. The direct bioelectrocatalysis in combination with a tunable efficiency and a high stability make this type of architecture a promising system for the construction of enzyme-based biosensors.

EXPERIMENTAL SECTION

Chemicals. MES (2-(*N*-morpholino)ethanesulfonic acid) buffer was purchased from Sigma-Aldrich (Taufkirchen, Germany), dehydrated calcium chloride, sodium dodecyl sulfate (SDS), iron(III) sulfate, and D-fructose were obtained from Fluka Analytics (Taufkirchen, Germany), and 85% phosphoric acid was provided by Merck (Darmstadt, Germany). They were used without further purification. Poly(2-methoxyaniline-5-sulfonic acid)-*co*-aniline polymer (PMSA1; Scheme 1) was synthesized as reported before.^{38,59} Millipore water (18 M Ω) was used for all types of measurements.

Enzyme Solution. FDH from *Gluconobacter japonicus* was provided by Sigma-Aldrich as a lyophilized powder containing additional salts and agents for stabilization. According to the provider, the purchased sample of 4.5 mg of FDH contained 5.1% protein. Therefore, a 0.5 mg of protein/mL stock solution was prepared after dissolving the lyophilizate in 0.5 mL of McIlvaine buffer (pH 4.5). The enzyme solution was used without further purification. Its specific activity—1186 U/mg of protein—was determined prior to the use as described by the provider: the principle of the activity test is based on ferricyanide reduction by FDH in the presence of fructose.¹⁹ The reaction is stopped by the addition of a solution containing phosphoric acid, SDS, and iron(III) sulfate. SDS denatures the enzyme and thus disables further reduction of ferricyanide. Iron(III) sulfate reacts with the reaction product (ferrocyanide) to Prussian blue, which is detected spectrophotometrically at 660 nm at room temperature.

Measurements in Solution. UV–Vis Spectroscopy. At first, PMSA1 and FDH were mixed successively in MES buffer (10 mM, pH 4.0–6.5). After mixing and addition of a constant amount of the substrate fructose, UV–vis spectra were collected in the absence and in the presence of 20 mM CaCl_2 . Since the reduction of polymers is accompanied by the appearance of a strong absorbance band at 408 nm, the absorbance increase in time was followed at this wavelength.

Afterward, the Lambert–Beer equation was used for the calculation of the corresponding reaction rates. The following concentrations were used: [PMSA1] = 40 $\mu\text{g/mL}$, [FDH] = 18 $\mu\text{g/mL}$, [fructose] = 100 mM (unless noted otherwise).

Cyclic Voltammetry. Previously cleaned rectangular ITO coated glass slides with surface resistivity 15–25 $\Omega \text{ sq}^{-1}$ (obtained from Sigma-Aldrich, Taufkirchen, Germany) were used as working electrodes. PMSA1 polymer, FDH, and fructose were mixed successively in 10 mM MES buffer in the absence and in the presence of 20 mM CaCl_2 ; afterward, cyclic voltammetry was applied to follow the reaction. The following concentrations were used: [PMSA1] = 40 $\mu\text{g/mL}$, [FDH] = 18 $\mu\text{g/mL}$, [fructose] = 100 mM (unless noted otherwise).

Construction of Polymer/Enzyme Films. For the preparation of polymer/enzyme films, the previously cleaned rectangular ITO coated glass slides and macroporous ITO (prepared by a direct coassembly of poly(methyl methacrylate) beads (PMMA) and indium tin hydroxide nanoparticles (nano-ITO) with subsequent calcination as described before^{10,60}) were initially incubated in buffer solutions of the PMSA1–FDH mixture (1.5 mg mL^{-1} PMSA1, 18 $\mu\text{g/mL}$ FDH; 10 mM MES with or without 20 mM CaCl_2 , pH 5.5) for 2 h. Afterward, the PMSA1/FDH electrode was dipped into the same buffer without enzyme and polymer to wash away the unbound material.

Instruments. Electrochemical measurements were performed at room temperature in a homemade 1 mL cell using an Ag/AgCl/1 M KCl reference (Biometra, Germany) and a platinum-wire counter electrode. Cyclic voltammetric experiments were carried out with a μ Autolab Type II device (Metrohm, The Netherlands). The scan rate was set to 5 mV s^{-1} . The potential range was chosen as between –0.4 and +0.4 V vs Ag/AgCl. Data analysis was performed using GPES software (General Purpose for Electrochemical System, Eco Chemie, Utrecht, The Netherlands). UV–vis measurements were carried out using an Evolution 300 spectrophotometer (Thermo Fischer Scientific, Germany).

AUTHOR INFORMATION

Corresponding Authors

*E-mail for D.S.: david.sarauli@cup.lmu.de.

*E-mail for F.L.: flisdat@th-wildau.de.

Notes

The authors declare no competing financial interest.

ACKNOWLEDGMENTS

Financial support by the BMBF of Germany (project 03IS22011) is gratefully acknowledged. D.F.-R. and K.P. are grateful to the German Research Foundation (DFG, Grant No. FA 839/3-1 and SPP 1613), the NIM cluster (DFG), the research networks “Solar Technologies Go Hybrid” and UMWELTnanoTECH (State of Bavaria). K.P. gratefully acknowledges funding from the Dr. Klaus Römer-Stiftung.

REFERENCES

- (1) Ates, M. *Mater. Sci. Eng. C-Mater. Biol. Appl.* **2013**, *33*, 1853–1859.
- (2) Fabiano, S.; Tran-Minh, C.; Piro, B.; Dang, L. A.; Pham, M. C.; Vittori, O. *Mater. Sci. Eng. C-Biomimetic Supramol. Syst.* **2002**, *21*, 61–67.
- (3) Jha, S. K.; Kanungo, M.; Nath, A.; D’Souza, S. F. *Biosens. Bioelectron.* **2009**, *24*, 2637–2642.

- (4) Nemzer, L. R.; Schwartz, A.; Epstein, A. J. *Macromolecules* **2010**, *43*, 4324–4330.
- (5) Cosnier, S. *Biosens. Bioelectron.* **1999**, *14*, 443–456.
- (6) Farace, G.; Vadgama, R. *Bioanalytical application of impedance analysis: Transducing in polymer-based biosensors and probes for living tissues*; Springer: Berlin, 2004; Springer Series on Chemical Sensors and Biosensors 2.
- (7) Katz, E.; Minko, S.; Halamek, J.; MacVittie, K.; Yancey, K. *Anal. Bioanal. Chem.* **2013**, *405*, 3659–3672.
- (8) Walcarius, A.; Kuhn, A. *Trac-Trends Anal. Chem.* **2008**, *27*, 593–603.
- (9) Ramanavicius, A.; Habermuller, K.; Csoregi, E.; Laurinavicius, V.; Schuhmann, W. *Anal. Chem.* **1999**, *71*, 3581–3586.
- (10) Sarauli, D.; Peters, K.; Xu, C.; Schulz, B.; Fattakhova-Rohlfing, D.; Lisdat, F. *ACS Appl. Mater. Interfaces* **2014**, *6*, 17887–17893.
- (11) Sarauli, D.; Xu, C. G.; Dietzel, B.; Schulz, B.; Lisdat, F. *J. Mater. Chem. B* **2014**, *2*, 3196–3203.
- (12) Schuhmann, W.; Zimmermann, H.; Habermuller, K. V.; Laurinavicius, V. *Faraday Discuss.* **2000**, *116*, 245–255.
- (13) Wang, X. J.; Sjoberg-Eerola, P.; Immonen, K.; Bobacka, J.; Bergelin, M. J. *Power Sources* **2011**, *196*, 4957–4964.
- (14) Kawai, S.; Goda-Tsutsumi, M.; Yakushi, T.; Kano, K.; Matsushita, K. *Appl. Environ. Microbiol.* **2013**, *79*, 1654–1660.
- (15) Nakashima, K.; Takei, H.; Adachi, O.; Shinagawa, E.; Ameyama, M. *Clin. Chim. Acta* **1985**, *151*, 307–310.
- (16) Cracknell, J. A.; Vincent, K. A.; Armstrong, F. A. *Chem. Rev.* **2008**, *108*, 2439–2461.
- (17) Gupta, A.; Singh, V. K.; Qazi, G. N.; Kumar, A. *J. Mol. Microbiol. Biotechnol.* **2001**, *3*, 445–456.
- (18) Tkac, J.; Svitel, J.; Vostiar, I.; Navratil, M.; Gemeiner, P. *Bioelectrochemistry* **2009**, *76*, 53–62.
- (19) Ameyama, M.; Shinagawa, E.; Matsushita, K.; Adachi, O. *J. Bacteriol.* **1981**, *145*, 814–823.
- (20) Kamitaka, Y.; Tsujimura, S.; Setoyama, N.; Kajino, T.; Kano, K. *Phys. Chem. Chem. Phys.* **2007**, *9*, 1793–1801.
- (21) Kawai, S.; Yakushi, T.; Matsushita, K.; Kitazumi, Y.; Shirai, O.; Kano, K. *Electrochem. Commun.* **2014**, *38*, 28–31.
- (22) Hu, Y. W.; Yang, T.; Li, Q. H.; Guan, Q.; Jiao, K. *Analyst* **2013**, *138*, 1067–1074.
- (23) Wang, X. X.; Yang, T.; Li, X. A.; Jiao, K. *Biosens. Bioelectron.* **2011**, *26*, 2953–2959.
- (24) Fiorito, P. A.; de Torresi, S. I. C. *Talanta* **2004**, *62*, 649–654.
- (25) Karyakin, A. A.; Bobrova, O. A.; Luckachova, L. V.; Karyakina, E. E. *Sens. Actuator B-Chem.* **1996**, *33*, 34–38.
- (26) Doan, T. C. D.; Ramaneti, R.; Baggerman, J.; van der Bent, J. F.; Marcelis, A. T. M.; Tong, H. D.; van Rijn, C. J. M. *Sens. Actuator B-Chem.* **2012**, *168*, 123–130.
- (27) Jaymand, M. *Prog. Polym. Sci.* **2013**, *38*, 1287–1306.
- (28) Jiang, Y.; Epstein, A. J. *J. Am. Chem. Soc.* **1990**, *112*, 2800–2801.
- (29) Liao, Y. Z.; Strong, V.; Chian, W.; Wang, X.; Li, X. G.; Kaner, R. B. *Macromolecules* **2012**, *45*, 1570–1579.
- (30) Malinauskas, A. J. *Power Sources* **2004**, *126*, 214–220.
- (31) Shieh, Y. T.; Jung, J. J.; Lin, R. H.; Yang, C. H.; Wang, T. L. *Electrochim. Acta* **2012**, *70*, 331–337.
- (32) Sarauli, D.; Tanne, J.; Xu, C. G.; Schulz, B.; Trnkova, L.; Lisdat, F. *Phys. Chem. Chem. Phys.* **2010**, *12*, 14271–14277.
- (33) Beissenhirtz, M. K.; Scheller, F. W.; Stocklein, W. F. M.; Kurth, D. G.; Moehwald, H.; Lisdat, F. *Angew. Chem.-Int. Ed.* **2004**, *43*, 4357–4360.
- (34) Dronov, R.; Kurth, D. G.; Moehwald, H.; Scheller, F. W.; Lisdat, F. *Electrochim. Acta* **2007**, *53*, 1107–1113.
- (35) Dronov, R.; Kurth, D. G.; Moehwald, H.; Scheller, F. W.; Lisdat, F. *Angew. Chem.-Int. Ed.* **2008**, *47*, 3000–3003.
- (36) Wegerich, F.; Turano, P.; Allegrozzi, M.; Moehwald, H.; Lisdat, F. *Langmuir* **2011**, *27*, 4202–4211.
- (37) Spricigo, R.; Dronov, R.; Lisdat, F.; Leimkuehler, S.; Scheller, F.; Wollenberger, U. *Anal. Bioanal. Chem.* **2009**, *393*, 225–233.
- (38) Sarauli, D.; Xu, C. G.; Dietzel, B.; Schulz, B.; Lisdat, F. *Acta Biomater.* **2013**, *9*, 8290–8298.
- (39) Hui, H. X.; Huang, D. S.; McArthur, D.; Nissen, N.; Boros, L. G.; Heaney, A. P. *Pancreas* **2009**, *38*, 706–712.
- (40) Yamada, Y.; Aida, K.; Uemura, T. *J. Biochem.* **1967**, *61*, 636–646.
- (41) Avouris, P.; Aizawa, M. In *Atomic and Nanometer-Scale Modification of Materials: Fundamentals and Applications*; Springer: Berlin, 1993; Vol. 239, pp 315–316.
- (42) Borrmann, T.; Dominis, A.; McFarlane, A. J.; Johnston, J. H.; Richardson, M. J.; Kane-Maguire, L. A. P.; Wallace, G. G. *J. Nanosci. Nanotechnol.* **2007**, *7*, 4303–4310.
- (43) Pornputtkul, Y.; Strounina, E. V.; Kane-Maguire, L. A. P.; Wallace, G. G. *Macromolecules* **2010**, *43*, 9982–9989.
- (44) Cho, S. I.; Lee, S. B. *Acc. Chem. Res.* **2008**, *41*, 699–707.
- (45) Kang, E. T.; Neoh, K. G.; Tan, K. L. *Prog. Polym. Sci.* **1998**, *23*, 277–324.
- (46) Lee, K.; Cho, S.; Park, S. H.; Heeger, A. J.; Lee, C. W.; Lee, S. H. *Nature* **2006**, *441*, 65–68.
- (47) MacDiarmid, A. G. *Angew. Chem.-Int. Ed.* **2001**, *40*, 2581–2590.
- (48) Strounina, E. V.; Shepherd, R.; Kane-Maguire, L. A. P.; Wallace, G. G. *Synth. Met.* **2003**, *135*, 289–290.
- (49) Amaya, T.; Saio, D.; Koga, S.; Hirao, T. *Macromolecules* **2010**, *43*, 1175–1177.
- (50) Moulton, S. E.; Pornputtkul, Y.; Kane-Maguire, L. A. P.; Wallace, G. G. *Aust. J. Chem.* **2007**, *60*, 159–166.
- (51) Sanchis, C.; Ghanem, M. A.; Salavagione, H. J.; Morallon, E.; Bartlett, P. N. *Bioelectrochemistry* **2011**, *80*, 105–113.
- (52) Dennany, L.; O'Reilly, E. J.; Innis, P. C.; Wallace, G. G.; Forster, R. J. *Electrochim. Acta* **2008**, *53*, 4599–4605.
- (53) Masdarolomoor, F.; Innis, P. C.; Wallace, G. G. *Electrochim. Acta* **2008**, *53*, 4146–4155.
- (54) Schubart, I. W.; Goebel, G.; Lisdat, F. *Electrochim. Acta* **2012**, *82*, 224–232.
- (55) Scherbahn, V.; Putze, M. T.; Dietzel, B.; Heinlein, T.; Schneider, J. J.; Lisdat, F. *Biosens. Bioelectron.* **2014**, *61*, 631–638.
- (56) Goebel, G.; Schubart, I. W.; Scherbahn, V.; Lisdat, F. *Electrochem. Commun.* **2011**, *13*, 1240–1243.
- (57) Xu, S.; Minteer, S. D. *ACS Catal.* **2014**, *4*, 2241–2248.
- (58) Katz, E.; Loetzbeyer, T.; Schlereth, D. D.; Schuhmann, W.; Schmidt, H.-L. *J. Electroanal. Chem.* **1994**, *373*, 189–200.
- (59) Sarauli, D.; Xu, C. G.; Dietzel, B.; Stiba, K.; Leimkuehler, S.; Schulz, B.; Lisdat, F. *Soft Matter* **2012**, *8*, 3848–3855.
- (60) Liu, Y. J.; Peters, K.; Mandmeier, B.; Mueller, A.; Fominykh, K.; Rathousky, J.; Scheu, C.; Fattakhova-Rohlfing, D. *Electrochim. Acta* **2014**, *140*, 108–115.